NeuroImage 186 (2019) 126–136

Contents lists available at ScienceDirect

NeuroImage

journal homepage: www.elsevier.com/locate/neuroimage

Targeting reduced neural oscillations in patients with schizophrenia by transcranial alternating current stimulation

Sangtae Ahn [a,b], Juliann M. Mellin [a,b], Sankaraleengam Alagapan [a,b], Morgan L. Alexander [a,b], John H. Gilmore [a], L. Fredrik Jarskog [a,c], Flavio Fröhlich [a,b,d,e,f,g,*]

[a] Department of Psychiatry, University of North Carolina at Chapel Hill, Chapel Hill, NC, 27599, United States
[b] Carolina Center for Neurostimulation, University of North Carolina at Chapel Hill, Chapel Hill, NC, 27599, United States
[c] North Carolina Psychiatric Research Center, Raleigh, NC, 27610, United States
[d] Department of Neurology, University of North Carolina at Chapel Hill, Chapel Hill, NC, 27599, United States
[e] Department of Biomedical Engineering, University of North Carolina at Chapel Hill, Chapel Hill, NC, 27599, United States
[f] Department of Cell Biology and Physiology, University of North Carolina at Chapel Hill, Chapel Hill, NC, 27599, United States
[g] Neuroscience Center, University of North Carolina at Chapel Hill, Chapel Hill, NC, 27599, United States

ARTICLE INFO

Keywords:
Electroencephalography
Alpha oscillation
Auditory steady-state response
Functional connectivity
Schizophrenia
Auditory hallucination

ABSTRACT

Transcranial alternating current stimulation (tACS) modulates endogenous neural oscillations in healthy human participants by the application of a low-amplitude electrical current with a periodic stimulation waveform. Yet, it is unclear if tACS can modulate and restore neural oscillations that are reduced in patients with psychiatric illnesses such as schizophrenia. Here, we asked if tACS modulates network oscillations in schizophrenia. We performed a randomized, double-blind, sham-controlled clinical trial to contrast tACS with transcranial direct current stimulation (tDCS) and sham stimulation in 22 schizophrenia patients with auditory hallucinations. We used high-density electroencephalography to investigate if a five-day, twice-daily 10Hz-tACS protocol enhances alpha oscillations and modulates network dynamics that are reduced in schizophrenia. We found that 10Hz-tACS enhanced alpha oscillations and modulated functional connectivity in the alpha frequency band. In addition, 10Hz-tACS enhanced the 40Hz auditory steady-state response (ASSR), which is reduced in patients with schizophrenia. Importantly, clinical improvement of auditory hallucinations correlated with enhancement of alpha oscillations and the 40Hz-ASSR. Together, our findings suggest that tACS has potential as a network-level approach to modulate reduced neural oscillations related to clinical symptoms in patients with schizophrenia.

1. Introduction

Neural oscillations are a fundamental mechanism that organizes the temporal relationship of activity patterns in large-scale brain networks. Several psychiatric disorders have been associated with impairment of neural oscillations (Uhlhaas and Singer, 2012). In particular, patients with schizophrenia exhibit reduced neural oscillations involved in sensory and cognitive processing (Uhlhaas and Singer, 2010). Therefore, strategies to target and modulate reduced neural oscillations may serve both as a tool to investigate the causal relationship between oscillation abnormalities and symptom manifestations and, ultimately, to therapeutic intervention to treat patients by restoring physiological oscillation dynamics. Transcranial alternating current stimulation (tACS) is a non-invasive brain stimulation modality that applies oscillating electrical currents to the brain via scalp electrodes. A single session of tACS enhances posterior alpha oscillations (8–12 Hz) in healthy humans (Helfrich et al., 2014; Vossen et al., 2015; Zaehle et al., 2010) and its effects outlast stimulation for about an hour (Kasten et al., 2016; Neuling et al., 2013). Yet, it has remained unknown if tACS, and in particular repeated application of tACS, can alter or modulate cortical networks in disorders associated with dysfunction of neural oscillations such as schizophrenia.

Auditory hallucinations are a major symptom of schizophrenia and are considered the consequence of aberrant hyperactivity in the left temporo-parietal junction (TPJ) (Silbersweig et al., 1995, 1994, 1993) and hypoactivity in the left dorsolateral prefrontal cortex (DLPFC) (Lawrie et al., 2002; Sanfilipo et al., 2000). Further support for this model is provided by findings of reduced functional connections between these two brain regions (Garrity et al., 2007; Lynall et al., 2010;

* Corresponding author. 115 Mason Farm Rd. NRB 4109F, Chapel Hill, NC, 27599, United States.
E-mail address: flavio_frohlich@med.unc.edu (F. Fröhlich).

https://doi.org/10.1016/j.neuroimage.2018.10.056
Received 2 May 2018; Received in revised form 1 October 2018; Accepted 21 October 2018
Available online 24 October 2018
1053-8119/© 2018 Elsevier Inc. All rights reserved.

Meyer-Lindenberg et al., 2001, 2005). In addition, patients with schizophrenia exhibit altered neural oscillations (Ford et al., 2007; Uhlhaas et al., 2008; Uhlhaas and Singer, 2010). In particular, reduced alpha oscillations are directly associated with symptoms of schizophrenia (Merrin and Floyd, 1992; Omori et al., 1995) and clinical improvement by antipsychotic medication such as clozapine is positively correlated with enhancement of alpha oscillations (Jin et al., 1995a; 1995b). In addition, resting-state alpha oscillations, which refer to fundamental network dynamics in the brain, are reduced in patients with schizophrenia (Hong et al., 2008; Miyauchi et al., 1990; Omori et al., 1995; Sponheim et al., 2000, 1997, 1994). Importantly, one study found reduced functional connectivity in resting-state between the frontal and temporal lobes (Hinkley et al., 2011). Motivated by these findings, we hypothesized that applying 10Hz-tACS to the left frontal and temporal lobes of patients with schizophrenia may modulate reduced alpha oscillations and functional connections between the two regions. To stimulate these two brain regions by in-phase tACS, we applied a three-electrode montage, which is a modified version of a previously used electrode montage for transcranial direct current stimulation (tDCS) studies for the treatment of auditory hallucinations in schizophrenia (Brunelin et al., 2012; Fröhlich et al., 2016).

The aim of this study was to target and modulate reduced neural oscillations in patients with schizophrenia by five days of 10Hz-tACS (with tDCS and sham stimulation conditions as controls). Specifically, we investigated target engagement of network oscillations by tACS with high-density electroencephalography (EEG) during two tasks (resting-state and auditory tasks). Clinical results for this study were recently reported elsewhere (Mellin et al., 2018). To our knowledge, we present the first target engagement study of repeated tACS application in schizophrenia.

2. Methods

2.1. Participants

This study was performed at the University of North Carolina at Chapel Hill (UNC—CH) (ClinicalTrials.gov, NCT02360228) and was approved by the Biomedical Institutional Review Board of UNC-CH. Participants were recruited from local clinics and academic medical centers. All participants met DSM-IV criteria for schizophrenia or schizoaffective disorder. Participants experienced at least three auditory hallucinations per week and were clinically stable as demonstrated by no hospitalizations for the past 3 months and stable antipsychotic medication dosing during participation (Table S1). Brief demographics and clinical assessments are tabulated (Table S2). Detailed information including inclusion/exclusion criteria and clinical analyses are described in a separate paper (Mellin et al., 2018). Data from 22 participants were analyzed.

2.2. Study design

This study was a randomized, double-blind, and sham-controlled clinical trial, with three stimulation conditions (10Hz-tACS, tDCS, and sham). Each participant was randomly assigned with equal probability to one of the three conditions. To achieve integrity of the double blinding, a researcher not involved in the study developed 5-digit random numbers and assigned the numbers to the participants. Each participant was randomized to one of the three stimulation conditions (e.g. 1: sham, 2: tACS, 3: tDCS) with the 5-digit numbers. One of the co-authors in the study wrote MATLAB scripts to deliver and control stimulation waveforms with the three stimulation conditions. This author was blinded to the 5-digit numbers and excluded from all stimulation sessions. The other two co-authors (study coordinators) performed all stimulation sessions with the 5-digit numbers for each participant. Further, the display on the stimulators was covered during stimulation to conceal information about the stimulation provided by the stimulators. All researchers were unaware of the condition assignments until all participants had completed the study. The auditory hallucination severity was measured by the auditory hallucination rating scale (AHRS) (Haddock et al., 1999). The AHRS was administered before the 1st stimulation on day 1 (baseline), after the 10th stimulation on day 5, and at the 1-week and 1-month follow-up study visits. A detailed description of the clinical data and analyses is provided in a separate paper (Mellin et al., 2018). EEG data were collected at the same time points with the exception of the recording on day 5, which was performed before stimulation to avoid contamination by potential instantaneous effects of stimulation on brain network dynamics. On day 5, EEG and the AHRS were not administered simultaneously but were spaced by the last stimulation session. We do not expect any large changes of the AHRS scores within less than an hour since the AHRS queries symptoms for a time window of several days. The sample size was determined by the amount of funding available for the grant that supported this work. The study was performed between June 2015 and February 2017.

2.3. Brain stimulation

We developed a custom-built interface in MATLAB and controlled two Neuroconn DC Plus stimulators (Neuroconn Ltd., Ilmenau, Germany) using “remote-mode” to ensure double-blind administration of stimulation. Our setup saved the applied stimulation waveform, which was validated offline by a lab member not otherwise involved in this study. The electrode montage was identical for all three stimulation conditions to ensure blinding of the research personnel to each stimulation condition. We applied three rubber electrodes to the scalp with Ten20 conductive paste (Bio-Medical Instruments, Clinton Township, MI). Each stimulator had two output connectors for electrode cables. One of the two outputs of each stimulator was connected together to form a common return path for the stimulation current through a 5 × 7cm electrode placed on Cz (center of the scalp). The other output of each stimulator was connected to a 5 × 5cm electrode placed between F3 and Fp1 (DLPFC) and between T3 and P3 (TPJ), respectively. For 10Hz-tACS, each 5 × 5cm electrode delivered an in-phase sinusoidal waveform with 1 mA amplitude. Both amplitude and phase of the stimulation waveforms were verified with an oscilloscope. For tDCS, the electrode between F3 and Fp1 delivered +2 mA amplitude current and the other electrode between T3 and P3 delivered -2 mA amplitude current. Stimulation montage and modeling of electric field distribution were calculated by the tES LAB 1.0 software (Neurophet Inc., Seoul, South Korea) as depicted in Fig. 1. We used these simulations of the electric field to determine the “stimulated” scalp locations for subsequent analysis of the EEG signal. Sham stimulation delivered 10 s of ramp-up, followed by 20 s of 10Hz-tACS, followed by 10 s of ramp-down for a total of 40 s. All participants completed twice-daily stimulation sessions for five consecutive days. Each stimulation session was 20 min long with a 3-h break between the two stimulation sessions. This structuring into two sessions per day was adopted from earlier work on tDCS for the treatment of auditory hallucinations (Brunelin et al., 2012). During stimulation, all participants were seated comfortably and watched a video of tropical fish (Undersea Productions, Queensland, Australia) to minimize the perception of phosphenes induced by stimulation. Participants were asked to watch the video and keep their eyes open.

2.4. EEG tasks

EEG data were recorded using a 128-channel Geodesic EEG system (EGI Inc., Eugene, OR) at a sampling rate of 1 kHz. Channel Cz and one channel between Cz and Pz were used as the reference and as the ground, respectively. All instructions and experimental tasks were implemented in Presentation (Neurobehavioral Systems, Inc., Berkeley, CA). Two experimental tasks were used. First, resting-state EEG data with eyes-open and eyes-closed were recorded for 8 min. Participants were instructed by a computer voice to fixate on a crosshair and open or close

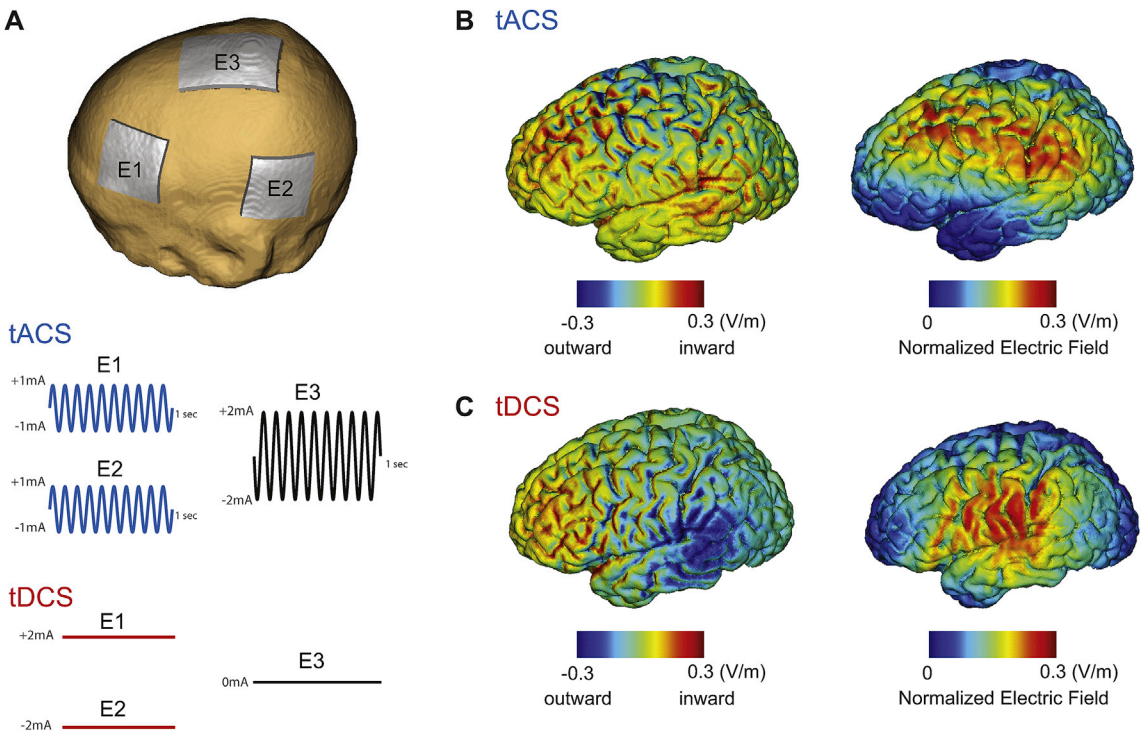

Fig. 1. Stimulation montage, waveforms, and electric field distribution. (A) Stimulation montage and waveforms for 10Hz-tACS and tDCS. Electrode E1 and E2 deliver in-phase waveforms (1 mA sine-wave) for 10Hz-tACS. For tDCS, electrode E1 and E2 deliver 2 mA (anode) and -2 mA (cathode) direct current, respectively. Electrode E3 was used as a return electrode for tACS. (B) Electric field distribution of inward/outward electric field (left) and normalized electric field (right) at the peak of the tACS waveform (C) Inward/outward electric field (left) and normalized electric field (right) for tDCS.

their eyes while staying relaxed. Eyes-closed and eyes-open conditions were alternated every 2 min and starting condition was randomized across the participants. We only present eyes-open data here since stimulation was applied in that state and we wanted to avoid confounds caused by the change in alpha oscillation strength due to eye closing. Second, the response to auditory click-trains was recorded. The auditory stimuli were delivered binaurally through air-conducting earphone tubes ER·3C (Etymotic Research Inc., Elk Grove Village, IL) at sound pressure level (SPL) of 90 dB. Participants fixated on a crosshair on a computer monitor while listening to 500 ms long click-trains at rates of 10Hz, 20Hz, 30Hz, 40Hz and 80Hz. This task was 15 min in length, separated into five 3-min blocks. Subsequent click-trains were separated by a jittered interval between 450 ms and 550 ms of silence. The order of the click-train frequencies was pseudo-random and balanced within each 3-min block, for a total of 200 click-trains per block and a grand total of 1000 click-trains. Synchronization between the auditory stimulus presentation and EEG acquisition was achieved by splitting the stereo output of the sound card into two separate mono outputs. One channel was used for the actual auditory stimuli while the other channel was recorded together with data.

2.5. EEG analysis and statistical testing

Offline processing was performed by EEGLAB (Delorme and Makeig, 2004), FieldTrip (Oostenveld et al., 2010), and custom-built scripts in MATLAB. First, all data were downsampled to 250Hz with anti-aliasing filtering (0.9π rad/sample cutoff and 0.2π rad/sample transition bandwidth) and band-pass filtered from 1 to 50Hz for the resting-state data, from 1 to 100Hz with 60Hz notch filter for the click-trains data. Second, the data were preprocessed by an artifact subspace reconstruction algorithm (Mullen et al., 2013) to identify high-variance data epochs and reconstruct missing data. Briefly, the algorithm first finds a minute of data that represents clean EEG signals that serve as a baseline. Then, principle component analysis is applied to the whole data set with a sliding window to find the subspaces in which there is activity that is more than five standard deviations away from the baseline EEG. Once the function has identified the outlier subspaces, it treats them as missing data and reconstructs their content using a mixing matrix that is calculated on the clean data. Third, bad channels that were found in the previous step were interpolated and common average referencing was performed. After then, infomax independent component analysis (ICA) (Jung et al., 2000) was performed to remove eye blinking, eye movement, muscle activity, and heartbeat artefact. All ICA components were visually inspected and noise components were manually selected for rejection. These initial pre-processing steps were carried out on the full EEG dataset before unblinding the study.

For the resting-state EEG, data were epoched into 2-s windows. Each epoch was visually inspected in the temporal domain and bad epochs that contained abnormal signal spikes or very pronounced fluctuations (larger than 100μV) due to head movement for all three conditions were removed (2.61 ± 1.1 of 120 trials). We found no significant difference of the rejected epochs between the three conditions (one-way ANOVA, $F_{2,19} = 0.65$, $p = 0.53$). Power spectral density (PSD) was computed by Welch's method with a 2-sec window and a 12.5% overlap resulting in a PSD with 0.5Hz frequency bins. Individual alpha frequency (IAF), which we defined as the frequency of the peak power in the occipital alpha band (8–12Hz) in the eye-closed condition, was selected for each participant. The power of alpha oscillations was determined by averaging of the PSD around the IAF ($IAF - 1Hz \leq IAF \leq IAF + 1Hz$) and the alpha oscillations were spatially normalized by the average of all channels to remove the inter-subject variability of alpha oscillations (Ahn et al., 2016, 2014). Thirty-eight channels outside of the scalp were excluded and the remaining 90 channels corresponding to scalp locations were used for topographical representation.

For statistical analysis, custom-built scripts in R (R Foundation for Statistical Computing, Vienna, Austria) were used. We adopted a linear mixed model analysis with fixed factors of "session" (baseline, day 5, 1-week, and 1-month) and "condition" (10Hz-tACS, tDCS, and sham), with

random factor "participant" to account for repeat measures within participants. We used the power of the alpha oscillations averaged across channels (41 channels, Fig. S3) in the stimulated regions (left hemisphere) as a dependent variable since we hypothesized that the left hemisphere was modulated by tACS or tDCS based on the electric field modeling (Fig. 1). Kenward-Roger approximations were used to obtain p-values and perform F-tests for each factor and their interaction. Post-hoc statistical tests were performed using student's t-test across participants at each channel and it was corrected by false discovery rate (FDR) (Benjamini and Hochberg, 1995) from the entire scalp channels. Changes of alpha oscillations over sessions were quantified with a modulation index, $(Alpha_{post} - Alpha_{base})/(Alpha_{post} + Alpha_{base})$ where $Alpha_{post}$ and $Alpha_{base}$ are alpha oscillations post-stimulation (day 5, 1-week, and 1-month) and at baseline (day 1 of stimulation), respectively.

To compute functional connectivity in terms of phase synchronization in the resting-state EEG data, we adopted a debiased weighted phase lag index (WPLI) to minimize the effects of volume conduction and noise originating from other scalp locations (Vinck et al., 2011). This method is also debiased in terms of sample size. We computed WPLI as

$$\Phi = \frac{|E\{|\Im\{X\}|sign(\Im\{X\})\}|}{E\{|\Im\{X\}|\}} \quad (1)$$

Here $\Im\{X\}$ denotes the imaginary component of the cross-spectrum. $E\{\cdot\}$ is the expected value operator and $sgn(\Im\{X\})$ indicates the sign of $\Im\{X\}$. $|\Im\{X\}|$ is the magnitude. Phase synchronization was computed with 0.5Hz frequency resolution for frequencies from 1 to 50Hz for all channel pairs on the scalp. For statistical testing in functional connectivity, we used the circular block bootstrapping (Politis and Romano, 1992) to preserve temporal dependencies in the time series. Block-length for each calculation was determined by a block-length algorithm (Politis and White, 2004). Each trial was resampled using the circular block bootstrapping with defined block-length. After constructing this surrogate data in this way 1000 times, only statistically significant WPLI values were extracted ($p < 0.05$). Global functional connectivity was obtained by averaging of all WPLI values for all scalp channels at each frequency (0.5Hz bin). The peak frequency was obtained by selecting a dominant peak in the frequency domain.

In the auditory task, EEG data were epoched from −0.1 to 0.5 s, resulting in 200 trials of click-trains for each frequency (10, 20, 30, 40 and 80Hz). Each epoch was visually inspected in time-domain and noisy epochs (8.8 ± 1.7 of 200 trials) for all three conditions were removed. We found no significant difference of the rejected epochs between the three conditions (one-way ANOVA, $F_{2,19} = 1.15$, $p = 0.33$). Time-frequency analysis was performed using Morlet wavelet transform (7 cycles). Amplitudes and phase information were obtained and inter-trial phase coherence (ITPC) of auditory steady-state response (ASSR) was computed using the phase information across trials as

$$\mathrm{ITPC(c,f,t)} = \left|\frac{1}{n}\sum_{e=1}^{n}\frac{X_e(c,f,t)}{|X_e(c,f,t)|}\right|, \quad (2)$$

where $X_e(c,f,t)$ is the spectral estimate of epoch e at channel c, frequency f, and time t (n=total number of epochs). We followed the same statistical approach with the resting-state EEG data and set averaged ITPC over significant activation regions by the auditory click-trains as a dependent variable. The topographical distribution of ITPC was computed by averaging from 0 to 0.5 s (stimulus duration) at each click-trains frequency. Post-hoc tests were performed using student's t-test across participant at each EEG channel.

3. Results

3.1. 10Hz-tACS enhances alpha oscillations

We first investigated if the five-day course of 10Hz-tACS modulated alpha oscillations by comparing the change in alpha oscillation power across the three study conditions (10Hz-tACS, tDCS, and sham). Using a mixed linear model, we found a significant interaction (session*condition) for the spatially-normalized alpha power averaged over the stimulated regions ($F_{6,57} = 3.49$, $p = 0.005$) but no main effect for session ($F_{3,63} = 1.59$, $p = 0.24$) or condition ($F_{2,19} = 2.48$, $p = 0.11$). Specifically, we found a significant interaction on day 5 ($F_{2,19} = 7.72$, $p = 0.003$) but no main effect for condition ($F_{2,19} = 0.18$, $p = 0.83$) and session ($F_{1,21} = 2.59$, $p = 0.12$). To investigate the changes of alpha power as a function of the stimulation condition on day 5, we next calculated the changes in spatially-normalized alpha power at each channel from baseline (day 1 of stimulation). For the 10Hz-tACS condition, we observed a significant increase of alpha power in the left temporal region on day 5 of stimulation (Fig. 2A, black dots indicate $p < 0.05$ with FDR correction). Power spectra on the left temporal region around individual alpha frequency are presented along with the topographies for all sessions. We further found a consistent increase of alpha power for the two follow-up sessions at 1-week and 1-month (Fig. 2A, second and third topographies), albeit statistical significance was not reached (no interaction effect, $F_{2,19} = 1.22$, $p = 0.31$ at 1-week and $F_{2,19} = 1.21$, $p = 0.32$ at 1-month). In contrast, we observed only minor changes of alpha power in the tDCS condition (Fig. 2B, no significant changes). In the sham condition, likewise, we found only minor changes of alpha power (Fig. 2C, no significant changes). These results indicate that 10Hz-tACS successfully enhanced alpha power in the left temporal region, close to the location of the stimulation electrodes. This enhancement remained visible for the two follow-up sessions but failed to reach statistical significance in the 10Hz-tACS condition.

3.2. 10Hz-tACS modulates functional connectivity

Reduced functional connectivity is one of the prominent network deficits in patients with schizophrenia (Lawrie et al., 2002; Vercammen et al., 2010). To examine modulation of functional connectivity determined from scalp-level EEG signals, we calculated WPLI between EEG channel pairs. Global functional connectivity averaged over the entire set of scalp channel pairs was calculated to minimize spurious findings of local functional connectivity. We determined global functional connectivity (1–50Hz) as a function of frequency with a 0.5Hz resolution (Fig. 3A, significant WPLI for all participants and sessions) and we found that the peak of the global functional connectivity strength was shifted to 10Hz only for 10Hz-tACS but not tDCS or sham stimulation (Fig. 3B, lines correspond to individual participants). This shift in the frequency of the functional connectivity was maintained for some participants at the 1-week follow-up, however, the peak frequency returned to the baseline frequency (from before stimulation) at the 1-month follow up for all participants. In contrast, the peak frequency of the global functional connectivity did not yield consistent changes over sessions in the tDCS and sham conditions (Fig. 3B, middle and bottom panels). The peak shift of global functional connectivity to 10Hz indicates that functional connections at 10Hz were enhanced by 10Hz-tACS and this finding implies that 10Hz-tACS successfully modulated network dynamics by enhancing phase synchronization in a frequency-specific way.

3.3. 10Hz-tACS enhances auditory steady-state responses

Deficits in auditory processing are commonly found in patients with schizophrenia who experience auditory hallucinations. Here, we investigated how our multi-session protocol of tACS changed the auditory response by measuring ITPC of the ASSR elicited by auditory click-trains. We examined ITPC for five different frequencies of auditory click-trains (10, 20, 30, 40, and 80Hz). In agreement with previous studies that found a preferential response to 40Hz click trains due to resonance in the human auditory system (Joliot et al., 1994), we found a consistent ASSR for 40Hz click-trains in central scalp locations (Fig. S1, baseline 40Hz-ASSR, no significant difference between the conditions). We also

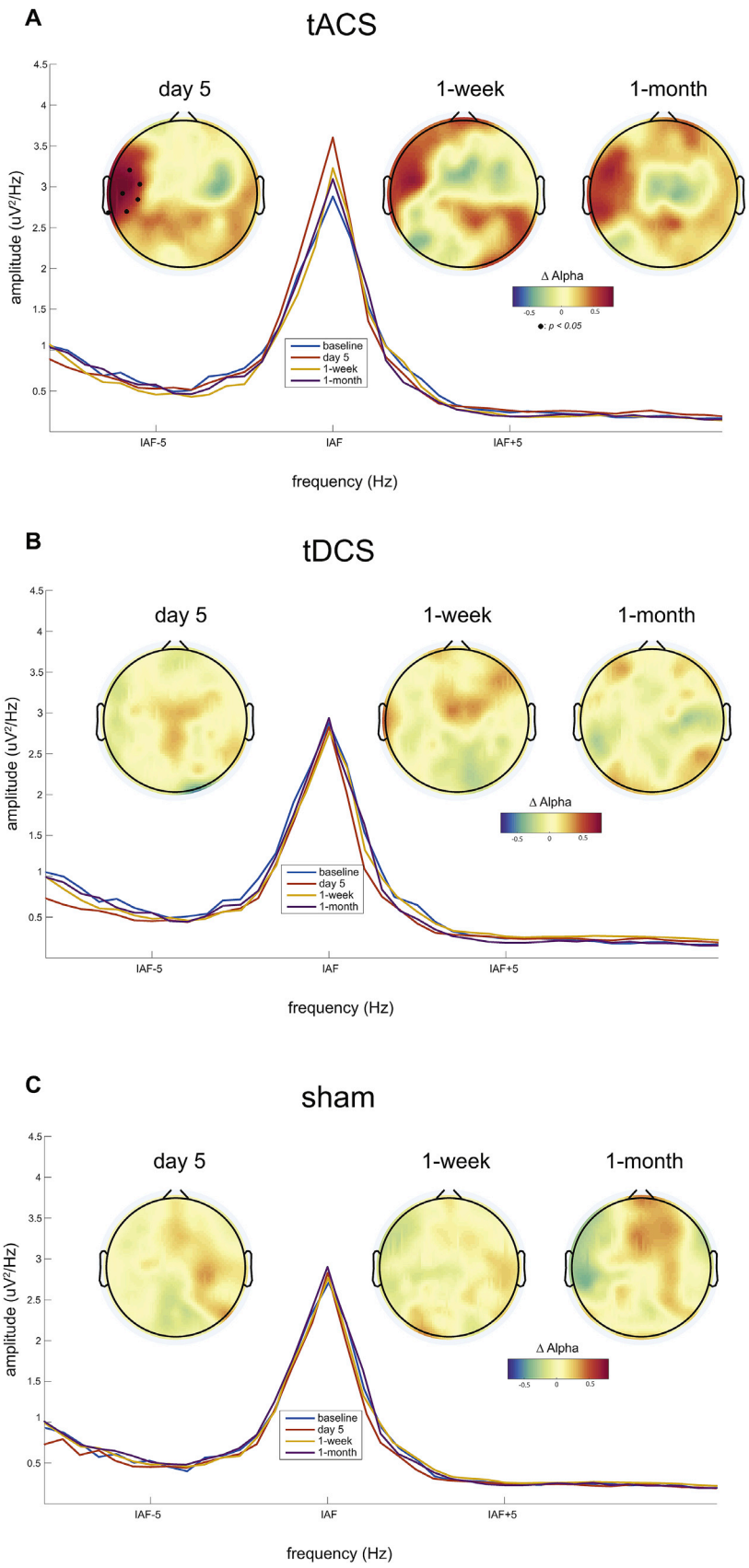

Fig. 2. Participant-averaged topographical distributions of changes in alpha power from baseline and power spectra in the left temporal region for all sessions. Individual alpha frequency was used (IAF±1Hz) for plotting topographies. Black dots in topography represent significant EEG channels from baseline ($p < 0.05$ with FDR correction).

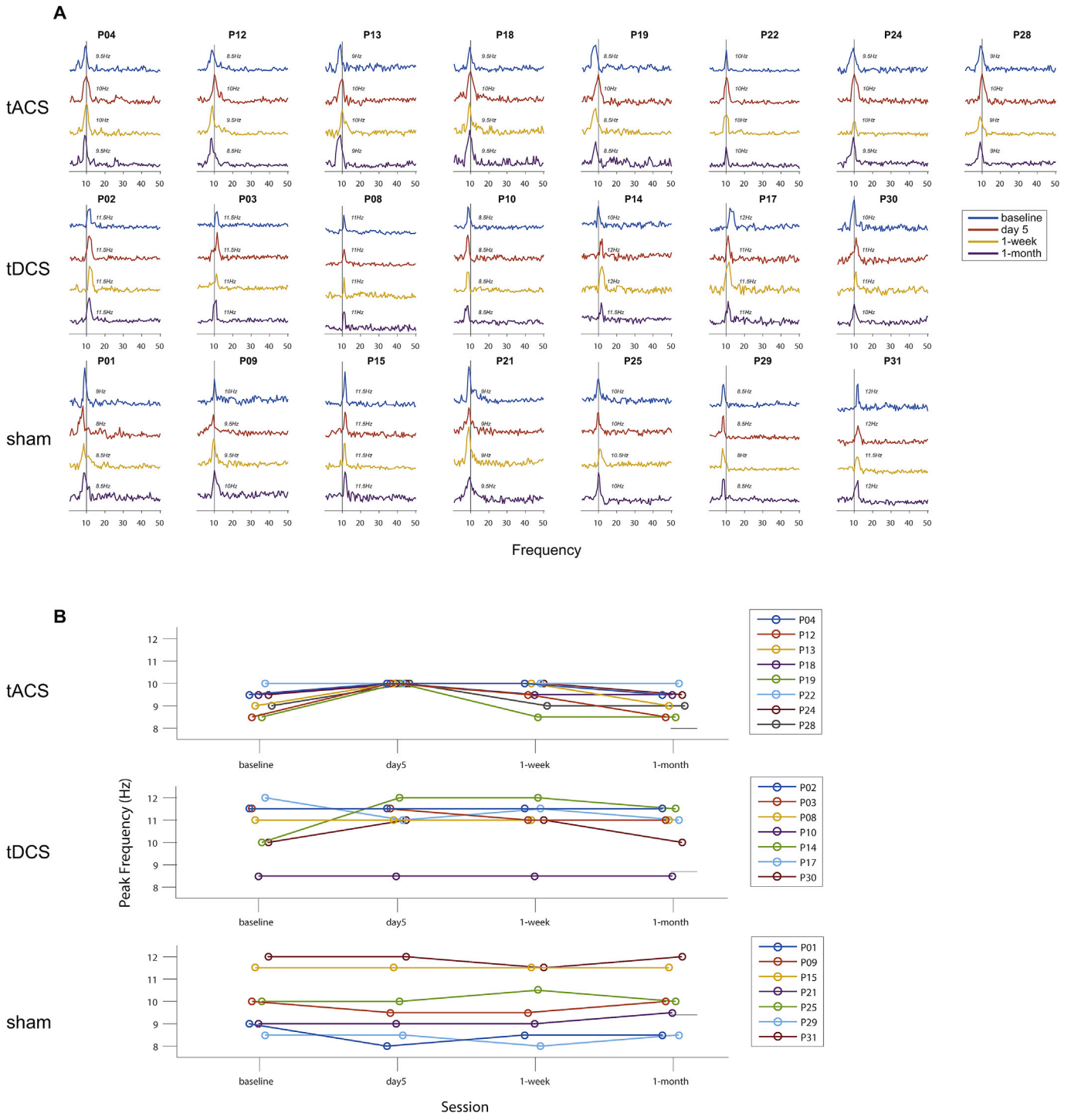

Fig. 3. Global functional connectivity by weighted phase lag index (WPLI). Statistically significant WPLI values with surrogates calculated by the circular bootstrapping (n = 1000, $p < 0.05$) were obtained over all channels on the scalp. (A) Traces of global functional connectivity from 1 to 50Hz with a 0.5Hz resolution for all participants and sessions. Each row and column indicate condition and individual participant, respectively. Four different colored lines represent sessions. (B) Individual peak frequencies are presented. Each row indicates stimulation condition. Lines represent individual participants.

examined ASSR for auditory stimulation at 10, 20, 30, and 80Hz. For 10Hz and 80Hz, no auditory response was found. Both 20Hz and 30Hz did show some degree of ASSR, which was not modulated by stimulation (Fig. S2). To examine if this ASSR changed as a function of session and condition, we used a linear mixed model with the ITPC of the response to 40Hz auditory stimulation as a dependent variable (averaged over time for the stimulus presentation duration (0–500 ms) and averaged over channels in the central region, Fig. S3). We found a significant interaction between session and condition ($F_{6,57} = 4.20$, $p = 0.001$) but no main effect for session ($F_{3,63} = 1.89$, $p = 0.14$) and condition ($F_{2,19} = 1.58$, $p = 0.23$). Specifically, we found a significant interaction on day 5 ($F_{2,19} = 6.77$, $p = 0.006$) but no main effect for condition ($F_{2,19} = 0.39$, $p = 0.68$) and session ($F_{1,21} = 0.91$, $p = 0.35$). To determine which stimulation condition mediated this interaction, we first calculated the topographical distributions of changes in the ASSR from baseline for each session and condition. We found that the 40Hz-ASSR was enhanced only

in the 10Hz-tACS condition (central region, Fig. 4A, top rows, black dots indicate significant channels, $p < 0.05$ with FDR correction). The enhancement gradually diminished over session and did not reach significance at the two follow-up sessions (no interaction effect, $F_{2,19} = 0.85$, $p = 0.44$ at 1-week and $F_{2,19} = 0.98$, $p = 0.39$ at 1-month, $p > 0.05$ for all channels). In contrast, topographical distributions for the tDCS and sham conditions did not yield an increased 40Hz-ASSR. In both cases, we observed slightly decreased 40Hz-ASSR that did not reach significance (Fig. 4A, middle and bottom rows). We then examined the time-course of the 40Hz-ASSR for the channels that exhibited a significant enhancement of the 40Hz-ASSR on day 5 in the tACS condition. The 40Hz-ASSR averaged across these channels was enhanced for the entire stimulus presentation duration (0–500 ms) on day 5 of stimulation (Fig. 4B, top row, significance map shown in Fig. S4). In contrast, we did not observe changes in the 40Hz-ASSR around 40Hz for the same set of channels in the tDCS and sham conditions (Fig. 4B, middle and bottom rows). These results show that 10Hz-tACS selectively enhanced the 40Hz-ASSR and thus suggest that enhancement of alpha oscillation power and functional connectivity contributes to a renormalization of auditory processing in patients with schizophrenia.

3.4. Enhanced alpha oscillations and 40Hz-ASSR are positively correlated

We found 10Hz-tACS significantly enhanced alpha oscillations and 40Hz-ASSR on day 5 compared to baseline. To investigate the relationship these two measures, we computed correlations across participants. Changes in alpha oscillations and 40Hz-ASSR were obtained by averaging over the significant channels (Fig. 2A) and averaged ITPC of 40Hz-ASSR across stimulus duration of auditory click-trains (0–500 ms) for the significant channels (Fig. 4A). We found a significant positive correlation on day 5 ($r = 0.4684$, $p < 0.01$) and at the 1-week follow-up ($r = 0.3857$, $p < 0.05$) (Fig. 5) for the complete participant pool (n = 22). The significance wore off at 1-month follow-up visit ($r = 0.3364$, $p > 0.05$). Although we pooled all participants to obtain the correlations due to relatively small sample size per group, we observed that all participants in tACS group have increased alpha oscillations and 40Hz-ASSR on day 5 compared to baseline. This finding indicates that 10Hz-tACS selectively enhanced alpha oscillations and 40Hz-ASSR and the relationship between the two is correlated.

3.5. AHRS and EEG are correlated

Given our findings that 10Hz-tACS significantly enhanced both alpha oscillation power and functional connectivity and the 40Hz-ASSR, we next examined the relationship between these changes in network dynamics and clinical improvement. From our study of the clinical results (Mellin et al., 2018), we found the highest effect size in the tACS condition at day 5 for AHRS (Fig. S5). Specifically, we asked how much the enhancement was correlated with changes in auditory hallucination symptoms measured by the AHRS. We calculated the Spearman's rho between AHRS scores and alpha oscillation power from all participants at each EEG channel on the scalp. We chose AHRS and EEG from day 1 of stimulation as a baseline and calculated changes from this baseline (AHRS: difference in raw score; alpha oscillations: modulation index). We found areas of significant, strong negative and positive correlation coefficients in the left temporo-parietal/frontal and in the central region in the tACS condition on day 5, respectively (Fig. 6A: Topographical correlation map with significant channels ($p < 0.05$) with FDR correction). Negative correlation coefficients indicate that the decrease of auditory hallucination symptoms was associated with an increase in alpha oscillation power. Scatter plots for the negative and positive correlations in the topographies are presented (Fig. S6). For both the 1-week and 1-month follow-up sessions, we observed weaker correlations that did not reach statistical significance (Fig. S7). These results suggest that changes of alpha oscillation power and auditory hallucinations are correlated in specific regions in the brain. Importantly, this relationship

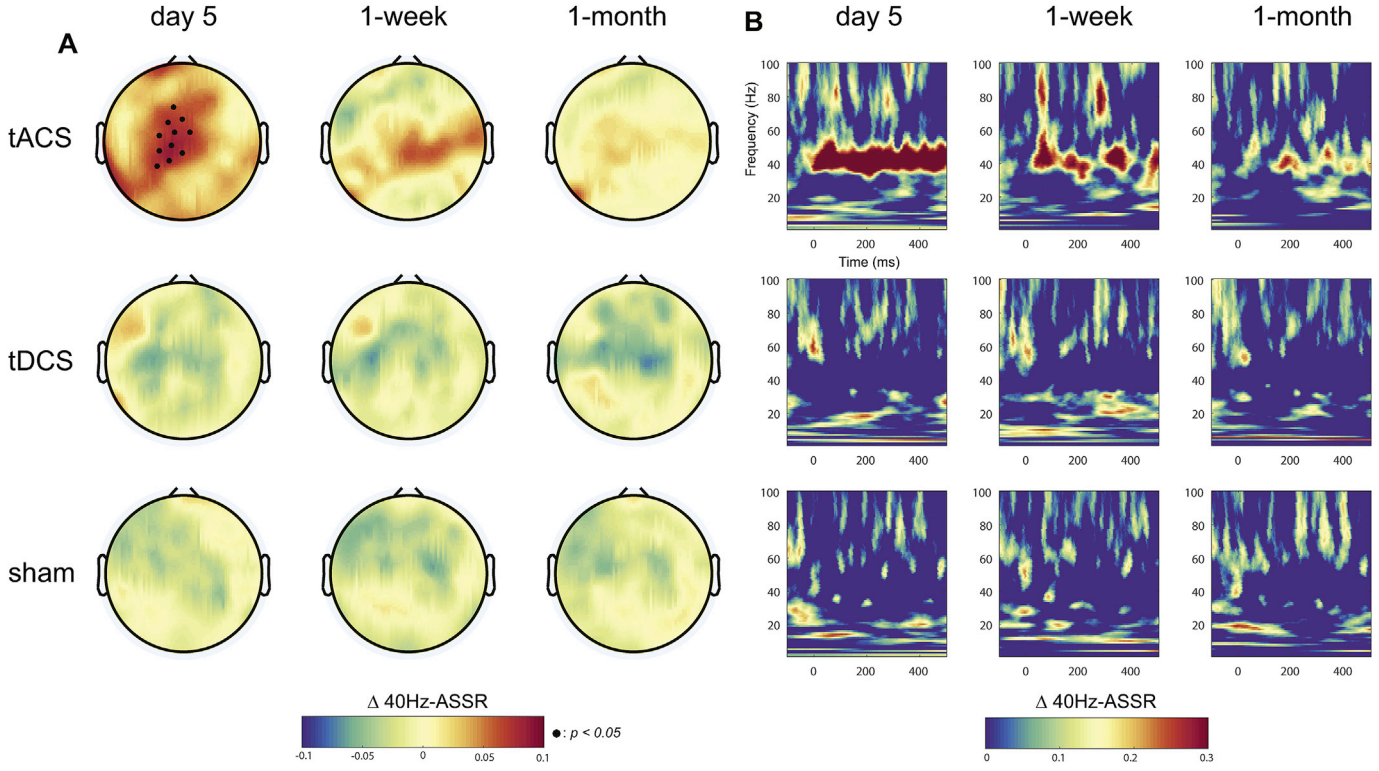

Fig. 4. Participant-averaged changes in 40Hz-ASSR. (A) Topographical distributions at 40Hz (0–500 ms) from baseline across each session and stimulation condition. Small black dots represent significant EEG channels ($p < 0.05$ with FDR correction). Each row and column indicate the stimulation condition and session, respectively. (B) Time-frequency map of the 40Hz-ASSR changes from baseline (channel-averaged over significant EEG channels in the central region).

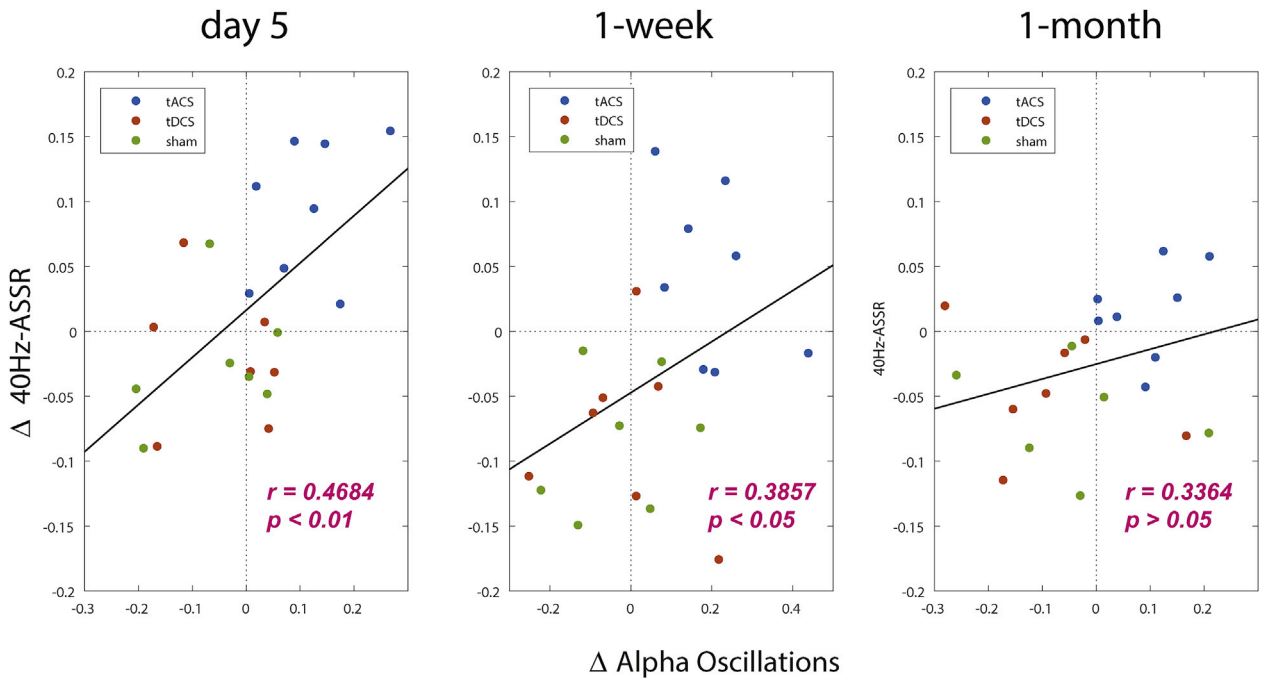

Fig. 5. Enhanced alpha oscillations and 40Hz auditory steady-state response (ASSR) are correlated for the complete participant pool (n = 22). Each dot indicates the participant and it is classified by different color scales. Alpha oscillations and 40Hz-ASSRs were obtained by averaged alpha oscillations across significant channels and averaged inter-trial phase coherence across stimulus time (0–500 ms) and significant channels, respectively.

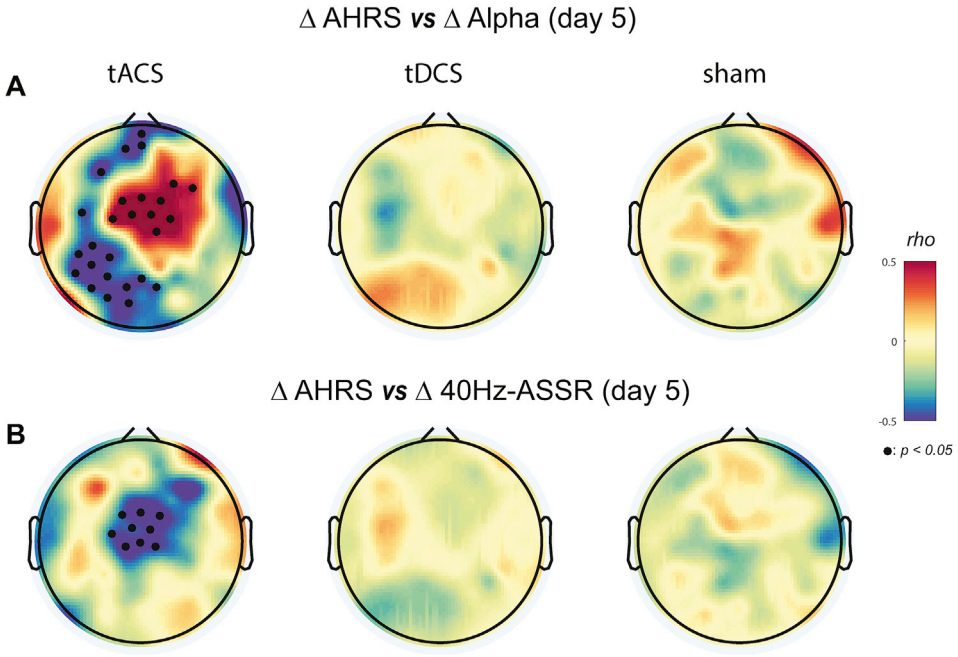

Fig. 6. Topographical distributions of correlations between EEG measures and auditory hallucination rating scale (AHRS). (A) Topographical correlation maps between changes in AHRS and alpha oscillation power for each stimulation condition on day 5 using the Spearman's rho. Small black dots indicate significant EEG channels ($p < 0.05$ with FDR correction). (B) Topographical correlation maps between changes in AHRS and the 40Hz-ASSR. Small black dots indicate significant EEG channels ($p < 0.05$ with FDR correction).

was strongest at the location of the stimulation electrodes. Second, we investigated the relationship between changes in AHRS and the 40Hz-ASSR. We calculated the Spearman's rho between changes in the AHRS and the 40Hz-ASSR across all participants (Fig. 6B). We found significant negative correlations over the central region ($p < 0.05$ with FDR correction) in the tACS condition on day 5 of stimulation. A scatter plot for the negative correlations is presented (Fig. S6). Thus, the reduction in auditory hallucination symptoms was accompanied by an increase in the 40Hz-ASSR over the central region, which is activated region of the 40Hz-ASSR. No significant correlations were obtained for the follow-up sessions (Fig. S8). These results suggest that the enhancement of the 40Hz-ASSR by 10Hz-tACS may represent a network-marker of symptom improvement.

4. Discussion

Recently, tACS was shown to successfully modulate endogenous alpha oscillations in healthy human participants (Helfrich et al., 2014; Kasten et al., 2016; Neuling et al., 2013; Vossen et al., 2015; Zaehle et al., 2010). However, the effect of tACS on reduced neural oscillations in

patients with psychiatric disorders was unknown. To address this question, we performed a randomized, double-blind, sham-controlled clinical trial that compared 10Hz-tACS to tDCS and sham stimulation in patients with schizophrenia experiencing persistent auditory hallucinations. We applied 10Hz-tACS to target reduced alpha oscillations and determine target engagement in terms of modulation of cortical oscillations measured by high-density EEG. In agreement with our hypothesis, we found that 10Hz-tACS enhanced alpha oscillations and modulated functional connectivity. In addition, 10Hz-tACS enhanced the 40Hz-ASSR, which is reduced in schizophrenia and associated with auditory processing deficits. The enhanced alpha oscillations and 40Hz-ASSR were correlated with reduction of auditory hallucinations for specific brain regions. Thus, our findings demonstrate that 10Hz-tACS successfully targets reduced neural oscillations but also has the potential to investigate abnormal neural oscillations by tACS in patients with schizophrenia.

While schizophrenia is often conceptualized as a network disorder, the cortical oscillations that have received the most attention tend to be in the higher frequencies such as gamma oscillations (Rutter et al., 2009; Spencer et al., 2003). We chose to target alpha oscillations instead since (1) previous studies reported reduced alpha oscillations in patients with schizophrenia compared to healthy participants (Hong et al., 2008; Miyauchi et al., 1990; Omori et al., 1995; Sponheim et al., 2000, 1997, 1994) and (2) we hypothesized that auditory hallucinations are the consequence of reduced functional connectivity in the fronto-parietal-temporal network (Hinkley et al., 2011). To our knowledge, the study presented here is the first study to examine a tACS paradigm for a psychiatric indication. Our stimulation protocol comprised 10 stimulation sessions with a total stimulation duration of 200 min. Previous investigations of target engagement of alpha oscillations by tACS have been limited to healthy control participants that received a single dose of tACS with typically lower stimulation amplitudes than what we used. Several but not all studies showed that such a stimulation session could enhance alpha oscillations during and immediately after stimulation (Helfrich et al., 2014; Kasten et al., 2016; Neuling et al., 2013; Vossen et al., 2015; Zaehle et al., 2010). No previous study has investigated longer-lasting effects on the time-scale of weeks as in our study. Although grand-averaged outlasting effects after one week did not reach significance, some participants with more persistent clinical improvement demonstrated outlasting effects on neural oscillations up to the final 1-month follow-up after 10Hz-tACS (Fig. S9). In addition, individual alpha frequency at baseline may be an indicator of inter-participant variability to outlasting effects but we could not find any relationship between individual alpha frequency and outcome measures (alpha power, ASSR, and AHRS).

Steady-state evoked potentials are a fundamental neural response to a temporally modulated stimulus in frequency and phase. ASSR has been widely investigated in patients with schizophrenia and consistent deficits specifically for the 40Hz-ASSR have been found in previous studies (Brenner et al., 2009; Krishnan et al., 2009; Kwon et al., 1999; Light et al., 2006; Spencer et al., 2008). Along with the 40Hz-ASSR, in this study, we also applied 10Hz, which is frequency-matched with 10Hz-tACS and harmonic frequencies; 20, 30, and 80Hz since no previous study has looked at modulation of ASSR at different frequencies by tACS. However, no clear ASSR was found for these other frequencies (data not shown). Strikingly, we found that 10Hz-tACS not only enhanced the 40Hz-ASSR but also is correlated with the reduction of AHRS scores. Thus, our results suggest that the 40Hz-ASSR could be a network marker to quantify the treatment response to 10Hz-tACS. Furthermore, this finding points to a fundamental, organizing role of alpha oscillations, which, when enhanced by stimulation, enable improvement of other, impaired network dynamics in other frequency bands.

This study has several limitations. First, the number of participants per condition was small and clinical improvement did not reach statistical significance (Mellin et al., 2018). However, effect size for change in AHRS is the greatest in the tACS condition (Mellin et al., 2018). Furthermore, the focus of the study was to identify target engagement for auditory hallucinations. In other words, changes in brain network dynamics in response to tACS appear to be a helpful tool to track the therapeutic effect of stimulation. A follow-up study with a larger sample size will provide the basis to address this question. Second, mean participant age differed between the conditions ($p = 0.01$, Table S2). We assessed Brief Assessment of Cognition in Schizophrenia (BACS) and found no significant differences ($p = 0.10$) in BACS scores at baseline between the groups. Although there is no known mechanism of how age might affect the response to brain stimulation in patients with schizophrenia, this will need to be addressed in future studies. Third, we did not collect EEG data during stimulation due to pronounced stimulation artifact. Although several previous studies investigated mathematical methods to remove these artifacts using principle component analysis (Helfrich et al., 2014) or a beamformer algorithm (Neuling et al., 2015), successful and complete removal of stimulation artifacts without distortion of the signals of interest remains to be demonstrated (Neuling et al., 2017; Noury and Siegel, 2017). Lastly, we examined global functional connectivity on the scalp channel pairs. This choice was motivated by our hypothesis that 10Hz-tACS not only enhances reduced alpha oscillations but also modulates disrupted network connections between brain regions. For this reason, we calculated functional connectivity across frequency and found the strongest connections are shifted to 10Hz in the tACS condition. We adopted global functional connectivity by averaging all scalp channels to minimize spurious local functional connectivity (Nolte et al., 2004; Stam et al., 2007; Vinck et al., 2011) since the activity of a single source in the brain is measureable in many EEG channels and one EEG channel likely represents averaged activity from multiple brain sources. In addition, different EEG channel locations across participants could hinder to obtain consistent local connectivity. Use of MRI and individually digitized EEG locations for each participant in an ongoing study will provide precise functional connectivity by source reconstruction.

In summary, we report successful target engagement of alpha oscillations by tACS in psychiatric patients. We successfully enhanced and modulated the neural oscillations. Further, the enhancement was correlated with reduction of symptoms measured by AHRS. These findings suggest that modulating and restoring reduced neural oscillations play a key role in reducing auditory hallucinations in patients with schizophrenia. Potentially, such targeted stimulation with tACS has therapeutic benefit for other psychiatric disorders associated with reduced neuronal oscillations such as major depressive disorder and autism spectrum disorder.

Conflicts of interest

Dr. Fröhlich is the lead inventor of IP filed by UNC. The clinical studies performed in the Frohlich Lab have received a designation as conflict of interest with administrative considerations. Dr. Fröhlich is the founder, CSO and majority owner of Pulvinar Neuro LLC, a company that markets research tDCS and tACS devices. Dr. Fröhlich has received research funding from the National Institutes of Health, the Brain Behavior Foundation, the Foundation of Hope, the Human Frontier Science Program, Tal Medical, and individual donations. Dr. Fröhlich is an adjunct professor in Neurology at the Insel Hospital of the University of Bern, Switzerland. Dr. Fröhlich receives royalties for his textbook Network Neuroscience published by Academic Press. Drs. Gilmore and Jarskog have received funding from the National Institutes of Health. Dr. Jarskog has received research support from Auspex/Teva, Boehringer Ingelheim, and Otsuka. Dr. Gilmore has no financial conflicts. Drs. Ahn and Alagapan have no financial conflicts. Juliann M. Mellin and Morgan L. Alexander have no financial conflicts.

Acknowledgements

The authors thank Kristen Sellers and Zhe Charles Zhou for their help with patient randomization for this study and Julianna Prim for editing

the manuscript. The authors specially thank Donghyeon Kim (Neurophet Inc.,) for providing valuable feedback on our stimulation montage and modeling of electric field distribution. This work was supported by the National Institute of Mental Health of the National Institutes of Health under Award Numbers R21MH105574, R01MH111889, and R01MH101547. The content is solely the responsibility of the authors and does not represent the official views of the National Institutes of Health.

Appendix A. Supplementary data

Supplementary data to this article can be found online at https://doi.org/10.1016/j.neuroimage.2018.10.056.

References

Ahn, S., Ahn, M., Cho, H., Chan Jun, S., 2014. Achieving a hybrid brain–computer interface with tactile selective attention and motor imagery. J. Neural. Eng. 11, 066004 https://doi.org/10.1088/1741-2560/11/6/066004.

Ahn, S., Nguyen, T., Jang, H., Kim, J.G., Jun, S.C., 2016. Exploring neuro-physiological correlates of drivers' mental fatigue caused by sleep deprivation using simultaneous EEG, ECG, and fNIRS data. Front. Hum. Neurosci. 10, 219. https://doi.org/10.3389/fnhum.2016.00219.

Benjamini, Y., Hochberg, Y., 1995. Controlling the false discovery rate: a practical and powerful approach to multiple testing. J. R. Stat. Soc. Ser. B 57, 289–300. https://doi.org/10.1111/j.2517-6161.1995.tb02031.x.

Brenner, C.A., Krishnan, G.P., Vohs, J.L., Ahn, W.-Y., Hetrick, W.P., Morzorati, S.L., O'Donnell, B.F., 2009. Steady state responses: electrophysiological assessment of sensory function in schizophrenia. Schizophr. Bull. 35, 1065–1077. https://doi.org/10.1093/schbul/sbp091.

Brunelin, J., Mondino, M., Gassab, L., Haesebaert, F., Gaha, L., Suaud-Chagny, M.-F., Saoud, M., Mechri, A., Poulet, E., 2012. Examining transcranial direct-current stimulation (tDCS) as a treatment for hallucinations in schizophrenia. Am. J. Psychiatry 169, 719–724. https://doi.org/10.1176/appi.ajp.2012.11071091.

Delorme, A., Makeig, S., 2004. EEGLAB: an open source toolbox for analysis of single-trial EEG dynamics including independent component analysis. J. Neurosci. Methods 134, 9–21. https://doi.org/10.1016/j.jneumeth.2003.10.009.

Ford, J.M., Krystal, J.H., Mathalon, D.H., 2007. Neural synchrony in schizophrenia: from networks to new treatments. Schizophr. Bull. 33, 848–852. https://doi.org/10.1093/schbul/sbm062.

Fröhlich, F., Burrello, T.N., Mellin, J.M., Cordle, A.L., Lustenberger, C.M., Gilmore, J.H., Jarskog, L.F., 2016. Exploratory study of once-daily transcranial direct current stimulation (tDCS) as a treatment for auditory hallucinations in schizophrenia. Eur. Psychiatr. 33, 54–60. https://doi.org/10.1016/j.eurpsy.2015.11.005.

Garrity, A.G., Pearlson, G.D., McKiernan, K., Lloyd, D., Kiehl, K.A., Calhoun, V.D., 2007. Aberrant "default mode" functional connectivity in schizophrenia. Am. J. Psychiatry 164, 450–457. https://doi.org/10.1176/ajp.2007.164.3.450.

Haddock, G., Carron, J., Tarrier, N., Faragher, E.B., 1999. Scales to measure dimensions of hallucinations and delusions: the psychotic symptom rating scales (PSYRATS). Psychol. Med. 29, 879–889.

Helfrich, R.F., Schneider, T.R., Rach, S., Trautmann-Lengsfeld, S.A., Engel, A.K., Herrmann, C.S., Ruffini, G., Miranda, P.C., Wendling, F., 2014. Entrainment of brain oscillations by transcranial alternating current stimulation. Curr. Biol. 24, 333–339. https://doi.org/10.1016/j.cub.2013.12.041.

Hinkley, L.B.N., Vinogradov, S., Guggisberg, A.G., Fisher, M., Findlay, A.M., Nagarajan, S.S., 2011. Clinical symptoms and alpha band resting-state functional connectivity imaging in patients with schizophrenia: implications for novel approaches to treatment. Biol. Psychiatry 70, 1134–1142. https://doi.org/10.1016/j.biopsych.2011.06.029.

Hong, L.E., Summerfelt, A., Mitchell, B.D., McMahon, R.P., Wonodi, I., Buchanan, R.W., Thaker, G.K., 2008. Sensory gating endophenotype based on its neural oscillatory pattern and heritability estimate. Arch. Gen. Psychiatry 65, 1008–1016. https://doi.org/10.1001/archpsyc.65.9.1008.

Jin, Y., Potkin, S.G., Sandman, C., 1995a. Clozapine increases EEG photic driving in clinical responders. Schizophr. Bull. 21, 263–268. https://doi.org/10.1093/schbul/21.2.263.

Jin, Y., Sandman, C.A., Wu, J.C., Bernat, J., Potkin, S.G., 1995b. Topographic analysis of EEG photic driving in normal and schizophrenic subjects. Clin. Electroencephalogr. 26, 102–107. https://doi.org/10.1177/155005949502600207.

Joliot, M., Ribary, U., Llinas, A.R., 1994. Human oscillatory brain activity near 40 Hz coexists with cognitive temporal binding. Neurobiology 91, 11748–11751. https://doi.org/10.1073/pnas.91.24.11748.

Jung, T.-P., Makeig, S., Humphries, C., Lee, T.-W., McKeown, M.J., Iragui, V., Sejnowski, T.J., 2000. Removing electroencephalographic artifacts by blind source separation. Psychophysiology 37, 163–178. https://doi.org/10.1111/1469-8986.3720163.

Kasten, F.H., Dowsett, J., Herrmann, C.S., 2016. Sustained aftereffect of alpha-tACS lasts up to 70 min after stimulation. Front. Hum. Neurosci. 10, 245. https://doi.org/10.3389/fnhum.2016.00245.

Krishnan, G.P., Hetrick, W.P., Brenner, C.A., Shekhar, A., Steffen, A.N., O'Donnell, B.F., 2009. Steady state and induced auditory gamma deficits in schizophrenia. Neuroimage 47, 1711–1719. https://doi.org/10.1016/j.neuroimage.2009.03.085.

Kwon, J.S., O'Donnell, B.F., Wallenstein, G.V., Greene, R.W., Hirayasu, Y., Nestor, P.G., Hasselmo, M.E., Potts, G.F., Shenton, M.E., McCarley, R.W., 1999. Gamma frequency–range abnormalities to auditory stimulation in schizophrenia. Arch. Gen. Psychiatr. 56, 1001–1005. https://doi.org/10.1001/archpsyc.56.11.1001.

Lawrie, S.M., Buechel, C., Whalley, H.C., Frith, C.D., Friston, K.J., Johnstone, E.C., 2002. Reduced frontotemporal functional connectivity in schizophrenia associated with auditory hallucinations. Biol. Psychiatry 51, 1008–1011. https://doi.org/10.1016/S0006-3223(02)01316-1.

Light, G.A., Hsu, J.L., Hsieh, M.H., Meyer-Gomes, K., Sprock, J., Swerdlow, N.R., Braff, D.L., 2006. Gamma band oscillations reveal neural network cortical coherence dysfunction in schizophrenia patients. Biol. Psychiatry 60, 1231–1240. https://doi.org/10.1016/j.biopsych.2006.03.055.

Lynall, M.-E., Bassett, D.S., Kerwin, R., McKenna, P.J., Kitzbichler, M., Muller, U., Bullmore, E., 2010. Functional connectivity and brain networks in schizophrenia. J. Neurosci. 30, 9477–9487. https://doi.org/10.1523/JNEUROSCI.0333-10.2010.

Mellin, J.M., Alagapan, S., Lustenberger, C., Lugo, C.E., Alexander, M.L., Gilmore, J.H., Jarskog, L.F., Fröhlich, F., 2018. Randomized trial of transcranial alternating current stimulation for treatment of auditory hallucinations in schizophrenia. Eur. Psychiatr. 51, 25–33. https://doi.org/10.1016/j.eurpsy.2018.01.004.

Merrin, E.L., Floyd, T.C., 1992. Negative symptoms and EEG alpha activity in schizophrenic patients. Schizophr. Res. 8, 11–20. https://doi.org/10.1016/0920-9964(92)90056-B.

Meyer-Lindenberg, A., Poline, J.-B., Kohn, P.D., Holt, J.L., Egan, M.F., Weinberger, D.R., Berman, K.F., 2001. Evidence for abnormal cortical functional connectivity during working memory in schizophrenia. Am. J. Psychiatry 158, 1809–1817. https://doi.org/10.1176/appi.ajp.158.11.1809.

Meyer-Lindenberg, A.S., Olsen, R.K., Kohn, P.D., Brown, T., Egan, M.F., Weinberger, D.R., Berman, K.F., 2005. Regionally specific disturbance of dorsolateral prefrontal–hippocampal functional connectivity in schizophrenia. Arch. Gen. Psychiatr. 62, 379. https://doi.org/10.1001/archpsyc.62.4.379.

Miyauchi, T., Tanaka, K., Hagimoto, H., Miura, T., Kishimoto, H., Matsushita, M., 1990. Computerized EEG in schizophrenic patients. Biol. Psychiatry 28, 488–494. https://doi.org/10.1016/0006-3223(90)90482-H.

Mullen, T., Kothe, C., Chi, Y.M., Ojeda, A., Kerth, T., Makeig, S., Cauwenberghs, G., Jung, Tzyy-Ping, 2013. Real-time modeling and 3D visualization of source dynamics and connectivity using wearable EEG. In: 2013 35th Annual International Conference of the IEEE Engineering in Medicine and Biology Society (EMBC). IEEE, pp. 2184–2187. https://doi.org/10.1109/EMBC.2013.6609968.

Neuling, T., Rach, S., Herrmann, C.S., 2013. Orchestrating neuronal networks: sustained after-effects of transcranial alternating current stimulation depend upon brain states. Front. Hum. Neurosci. 7, 161. https://doi.org/10.3389/fnhum.2013.00161.

Neuling, T., Ruhnau, P., Fuscà, M., Demarchi, G., Herrmann, C.S., Weisz, N., 2015. Friends, not foes: magnetoencephalography as a tool to uncover brain dynamics during transcranial alternating current stimulation. Neuroimage 118, 406–413. https://doi.org/10.1016/j.neuroimage.2015.06.026.

Neuling, T., Ruhnau, P., Weisz, N., Herrmann, C.S., Demarchi, G., 2017. Faith and oscillations recovered: on analyzing EEG/MEG signals during tACS. Neuroimage 147, 960–963. https://doi.org/10.1016/j.neuroimage.2016.11.022.

Nolte, G., Bai, O., Wheaton, L., Mari, Z., Vorbach, S., Hallett, M., 2004. Identifying true brain interaction from EEG data using the imaginary part of coherency. Clin. Neurophysiol. 115, 2292–2307. https://doi.org/10.1016/j.clinph.2004.04.029.

Noury, N., Siegel, M., 2017. Phase properties of transcranial electrical stimulation artifacts in electrophysiological recordings. Neuroimage 158, 406–416. https://doi.org/10.1016/j.neuroimage.2017.07.010.

Omori, M., Koshino, Y., Murata, T., Murata, I., Nishio, M., Sakamoto, K., Horie, T., Isaki, K., 1995. Quantitative EEG in never-treated schizophrenic patients. Biol. Psychiatry 38, 303–309. https://doi.org/10.1016/0006-3223(95)00300-6.

Oostenveld, R., Fries, P., Maris, E., Schoffelen, J.-M., 2010. FieldTrip: open source software for advanced analysis of MEG, EEG, and invasive electrophysiological data. Comput. Intell. Neurosci. 2011, 156869. https://doi.org/10.1155/2011/156869.

Politis, D.N., Romano, J.P., 1992. A Circular Block-resampling Procedure for Stationary Data, Exploring the Limits of Bootstrap. John Wiley & Sons, New York.

Politis, D.N., White, H., 2004. Automatic block-length selection for the dependent bootstrap. Econom. Rev. 23, 53–70. https://doi.org/10.1081/ETC-120028836.

Rutter, L., Carver, F.W., Holroyd, T., Nadar, S.R., Mitchell-Francis, J., Apud, J., Weinberger, D.R., Coppola, R., 2009. Magnetoencephalographic gamma power reduction in patients with schizophrenia during resting condition. Hum. Brain Mapp. 30, 3254–3264. https://doi.org/10.1002/hbm.20746.

Sanfilipo, M., Lafargue, T., Rusinek, H., Arena, L., Loneragan, C., Lautin, A., Feiner, D., Rotrosen, J., Wolkin, A., 2000. Volumetric measure of the frontal and temporal lobe regions in schizophrenia. Arch. Gen. Psychiatr. 57, 471–480. https://doi.org/10.1001/archpsyc.57.5.471.

Silbersweig, D.A., Stern, E., Frith, C., Cahill, C., Holmes, A., Grootoonk, S., Seaward, J., McKenna, P., Chua, S.E., Schnorr, L., Jones, T., Frackowiak, R.S.J., 1995. A functional neuroanatomy of hallucinations in schizophrenia. Nature 378, 176–179. https://doi.org/10.1038/378176a0.

Silbersweig, D.A., Stern, E., Frith, C.D., Cahill, C., Schnorr, L., Grootoonk, S., Spinks, T., Clark, J., Frackowiak, R., Jones, T., 1993. Detection of thirty-second cognitive activations in single subjects with positron emission tomography: a new low-dose $H_2{}^{15}O$ regional cerebral blood flow three-dimensional imaging technique. J. Cerebr. Blood Flow Metabol. 13, 617–629. https://doi.org/10.1038/jcbfm.1993.80.

Silbersweig, D.A., Stern, E., Schnorr, L., Frith, C.D., Ashburner, J., Cahill, C., Frackowiak, R.S.J., Jones, T., 1994. Imaging transient, randomly occurring neuropsychological events in single subjects with positron emission tomography: an event-related count rate correlational analysis. J. Cerebr. Blood Flow Metabol. 14, 771–782. https://doi.org/10.1038/jcbfm.1994.98.

Spencer, K.M., Nestor, P.G., Niznikiewicz, M.A., Salisbury, D.F., Shenton, M.E., McCarley, R.W., 2003. Abnormal neural synchrony in schizophrenia. J. Neurosci. 23, 7407–7411. https://doi.org/10.1523/JNEUROSCI.23-19-07407.2003.

Spencer, K.M., Salisbury, D.F., Shenton, M.E., McCarley, R.W., 2008. γ-Band Auditory steady-state responses are impaired in first episode psychosis. Biol. Psychiatry 64, 369–375. https://doi.org/10.1016/j.biopsych.2008.02.021.

Sponheim, S.R., Clementz, B.A., Iacono, W.G., Beiser, M., 2000. Clinical and biological concomitants of resting state EEG power abnormalities in schizophrenia. Biol. Psychiatry 48, 1088–1097. https://doi.org/10.1016/S0006-3223(00)00907-0.

Sponheim, S.R., Clementz, B.A., Iacono, W.G., Beiser, M., 1994. Resting EEG in first-episode and chronic schizophrenia. Psychophysiology 31, 37–43. https://doi.org/10.1111/j.1469-8986.1994.tb01023.x.

Sponheim, S.R., Iacono, W.G., Clementz, B.A., Beiser, M., 1997. Season of birth and electroencephalogram power abnormalities in schizophrenia. Biol. Psychiatry 41, 1020–1027. https://doi.org/10.1016/S0006-3223(96)00184-9.

Stam, C.J., Nolte, G., Daffertshofer, A., 2007. Phase lag index: assessment of functional connectivity from multi channel EEG and MEG with diminished bias from common sources. Hum. Brain Mapp. 28, 1178–1193. https://doi.org/10.1002/hbm.20346.

Uhlhaas, P.J., Haenschel, C., Nikolic, D., Singer, W., 2008. The role of oscillations and synchrony in cortical networks and their putative relevance for the pathophysiology of schizophrenia. Schizophr. Bull. 34, 927–943. https://doi.org/10.1093/schbul/sbn062.

Uhlhaas, P.J., Singer, W., 2012. Neuronal dynamics and neuropsychiatric disorders: toward a translational paradigm for dysfunctional large-scale networks. Neuron 75, 963–980. https://doi.org/10.1016/j.neuron.2012.09.004.

Uhlhaas, P.J., Singer, W., 2010. Abnormal neural oscillations and synchrony in schizophrenia. Nat. Rev. Neurosci. 11, 100–113. https://doi.org/10.1038/nrn2774.

Vercammen, A., Knegtering, H., den Boer, J.A., Liemburg, E.J., Aleman, A., 2010. Auditory hallucinations in schizophrenia are associated with reduced functional connectivity of the temporo-parietal area. Biol. Psychiatry 67, 912–918. https://doi.org/10.1016/j.biopsych.2009.11.017.

Vinck, M., Oostenveld, R., Van Wingerden, M., Battaglia, F., Pennartz, C.M.A., 2011. An improved index of phase-synchronization for electrophysiological data in the presence of volume-conduction, noise and sample-size bias. Neuroimage 55, 1548–1565. https://doi.org/10.1016/j.neuroimage.2011.01.055.

Vossen, A., Gross, J., Thut, G., 2015. Alpha power increase after transcranial alternating current stimulation at alpha frequency (α-tACS) reflects plastic changes rather than entrainment. Brain Stimul 8, 499–508. https://doi.org/10.1016/j.brs.2014.12.004.

Zaehle, T., Rach, S., Herrmann, C.S., Schurmann, M., Marshall, L., 2010. Transcranial Alternating Current Stimulation Enhances Individual Alpha Activity in Human EEG. PLoS One 5, e13766. https://doi.org/10.1371/journal.pone.0013766.